Published in final edited form as:
J Neurochem. 2007 December ; 103(5): 1968–1981. doi:10.1111/j.1471-4159.2007.04882.x.

Developmental mercury exposure elicits acute hippocampal cell death, reductions in neurogenesis, and severe learning deficits during puberty

Anthony Falluel-Morel[*], **Katie Sokolowski**[*], **Helene M. Sisti**[†], **Xiaofeng Zhou**[*], **Tracey J. Shors**[†], and **Emanuel DiCicco-Bloom**[*,‡]

[*]Department of Neuroscience and Cell Biology, UMDNJ-Robert Wood Johnson Medical School, Piscataway, New Jersey, USA

[†]Department of Psychology, Rutgers University, Piscataway, New Jersey, USA

[‡]Department of Pediatrics; Member of the Cancer Institute of New Jersey, New Jersey, USA

Abstract

Normal brain development requires coordinated regulation of several processes including proliferation, differentiation, and cell death. Multiple factors from endogenous and exogenous sources interact to elicit positive as well as negative regulation of these processes. In particular, the perinatal rat brain is highly vulnerable to specific developmental insults that produce later cognitive abnormalities. We used this model to examine the developmental effects of an exogenous factor of great concern, methylmercury (MeHg). Seven-day-old rats received a single injection of MeHg (5 μg/gbw). MeHg inhibited DNA synthesis by 44% and reduced levels of cyclins D1, D3, and E at 24 h in the hippocampus, but not the cerebellum. Toxicity was associated acutely with caspase-dependent programmed cell death. MeHg exposure led to reductions in hippocampal size (21%) and cell numbers 2 weeks later, especially in the granule cell layer (16%) and hilus (50%) of the dentate gyrus defined stereologically, suggesting that neurons might be particularly vulnerable. Consistent with this, perinatal exposure led to profound deficits in juvenile hippocampal-dependent learning during training on a spatial navigation task. In aggregate, these studies indicate that exposure to one dose of MeHg during the perinatal period acutely induces apoptotic cell death, which results in later deficits in hippocampal structure and function.

Keywords

cell cycle; hippocampus; learning; methylmercury; neurogenesis; programmed cell death

Normal development and function of the brain require a fine balance among several dynamic cellular processes including proliferation, differentiation, and cell death. The regulation of these processes depends on interactions among multiple factors from both endogenous and exogenous sources (Jacobson 1991; Vaccarino *et al*. 1999; Adams *et al*. 2000; Kandel *et al*. 2000; Rice and Barone 2000; DiCicco-Bloom and Sondell 2005). Such factors may exhibit region-specific effects in distinct brain structures, depending on both their developmental stage and respective responsiveness or vulnerability. Previous studies performed with basic fibroblast growth factor demonstrated that a single perturbation of

Address Correspondence and reprint requests to Emanuel DiCicco-Bloom, Department of Neuroscience & Cell Biology, Robert Wood Johnson Medical School, 675 Hoes Lane, Room RWJSPH 362, Piscataway, NJ 08854, USA. diciccem@umdnj.edu.

brain development during a sensitive period has both acute and long-term consequences on brain structure and function (Tao *et al*. 1996; Wagner *et al*. 1999; Cheng *et al*. 2001, 2002). Similarly, other studies of the perinatal rat brain demonstrate highly selective temporal vulnerabilities to specific developmental insults that lead to later cognitive deficits, and remarkable efficacy of basic fibroblast growth factor treatment to reduce damage and promote tissue and functional recovery (Kolb and Cioe 2000; Monfils *et al*. 2005). We took advantage of this informative system to examine the effects of an exogenous factor of great concern, methylmercury (MeHg), during this critical period. MeHg is a well known and potent neurotoxicant, with high level exposures during development leading to mental retardation, cerebral palsy, and seizures (Myers and Davidson 2000; Stein *et al*. 2002; Spurgeon 2006). However, while the deleterious effects of MeHg on brain development have been well described, far less is known about the specific cellular and molecular processes whose disruption in the living animal underlies brain pathogenesis.

In the present study, we investigated the effects of a single exposure to MeHg (5 μg/gbw) in 7-day-old rat pups. This dose is commonly used to study mercury neurotoxicity and leads to brain mercury levels around 500 ppb (ppb = ng/g; Lewandowski *et al*. 2002; Burke *et al*. 2006; Stringari *et al*. 2006). Although this dose produces acutely brain levels slightly higher than what is found in the general and primarily fish eating human population that live on volcanic islands (where brain Hg levels are ≤ 400 ppb; Lapham *et al*. 1995), it is much lower than that found with poisoning, resulting usually from non-lethal industrial accidents and manifesting as ataxia, perceptual deficits or insanity (> 1000 ppb) (Choi *et al*. 1978). Thus this model ensures we can reliably induce a cascade of detectable developmental changes that may serve as useful pathogenetic markers.

In this study, we hypothesized that exposure to one dose of MeHg would lead to changes in proliferation and cell death, especially in regions known to be involved in ongoing developmental neurogenesis, such as the hippocampus. It was further hypothesized that the consequent malformations would thereby impair processes related to learning and memory during puberty. Importantly, we expected this single injection paradigm would allow us to define the sequence of events that occur following MeHg exposure, leading to the identification of underlying mechanisms, a task that would have been far more complex using a chronic exposure paradigm where primary and secondary events would be potentially indistinguishable. Hopefully, by defining cellular and molecular mechanisms by which mercury alters brain development in neonatal rat, we may identify molecular markers and possible therapeutic targets suitable for further studies with relevance for human exposure.

Materials and methods

Animals

Female Sprague–Dawley rats with 4-day-old pups (P4) were purchased from Hilltop Lab Animals (Philadelphia, PA, USA). They were housed in a temperature-and light-controlled animal care facility and given food and water *ad libitum*. The body weight of the rat pups was monitored during treatments (Table 1). P7 rats were injected subcutaneously (s.c.) with vehicle or MeHg (2.5–10 μg/gbw) in a 50–100 μL bolus. Male and female pups were used, and no differences in response to perinatal MeHg exposure were observed at the ages when experiments were performed. All animal procedures were approved by the Robert Wood Johnson Medical School institutional animal care and utilization committee and conformed to NIH Guidelines for animal use.

Materials

Methylmercury chloride (CH_3HgCl) was purchased from Sigma (St Louis, MO, USA). A 1.5 mg/mL stock solution in 0.1 mol/L phosphate-buffered saline (PBS) was prepared immediately before use and dissolved by agitation. Bromodeoxyuridine (BrdU), a thymidine analog, was used to identify cells in S phase. Animals were injected i.p. with BrdU (100 μg/gbw; Sigma) 6 h after the treatment with MeHg. The pan-caspase inhibitor carbobenzoxy-valyl-alanyl-aspartyl-[*O*-methyl]-fluoromethylketone (Z-VAD-FMK) was obtained from R&D System (Minneapolis, MN, USA) and dissolved in dimethylsulfoxide. After dilution in culture medium, final concentrations of dimethylsulfoxide did not exceed 0.5%, and control cells were treated with the same vehicle.

[^{3}H]-thymidine incorporation

Tritiated thymidine (5 μCi/gbw; Amersham Bioscience, UK) was injected s.c. into animals 2 h prior to analysis. DNA synthesis was evaluated using a 'percent incorporation' assay, as described (Wagner *et al.* 1999; Cheng *et al.* 2002; Burke *et al.* 2006). Frozen tissues were manually homogenized in distilled water using a 22 gauge needle and syringe. An aliquot was removed for determination of total isotope uptake into the tissue. In an equal aliquot, DNA was precipitated with 10% trichloroacetic acid (TCA), sedimented by centrifugation (2700 *g*, 4°C, 15 min), and washed by resuspension and resedimentation. The final pellet was dissolved and counted along with the original aliquot in a scintillation spectrophotometer. As radiolabel incorporation into DNA depends on the amount of label taken up by the tissue, incorporation was calculated as the fraction of total tissue uptake. This method assures that experimental effects do not reflect possible differences in tissue region dissection or individual animal injection, absorption or blood flow, but rather changes in specific regional DNA synthesis.

Immunohistochemistry

Animals were perfused with 0.9% NaCl followed by 4% *p*-formaldehyde in 0.1 mol/L PBS. Brains were post-fixed in 4% *p*-formaldehyde in PBS for 12 h at 4°C, cryoprotected in 30% sucrose in PBS and cut, after embedding in Tissue-Tek (Sakura, Tokyo, Japan), into 12-lm thick coronal sections on a cryostat (Leica, Heidelberg, Germany). Sections were incubated in boiling 0.01 mol/L citrate buffer (3 × 30 min), hydrogen peroxide (0.3% in methanol, 10 min), 5% normal serum for 1 h, followed by primary antibody overnight at 4°C in 0.5% Triton X-100 and 1% normal serum in PBS. Primary antibodies used were rabbit antibody to cleaved-caspase 3 (1 : 200; Cell Signaling, Beverly, MA, USA), and mouse antibody to BrdU (1 : 100; Becton-Dickinson, San Jose, CA, USA). For single staining, biotinylated goat anti-rabbit or anti-mouse IgG (Vector Laboratories, Burlingame, CA, USA) was applied as second antibodies and avidin–biotin peroxidase complex (ABC kit; Vector Laboratories) served as amplification reagent. Diaminobenzidine served as chromogen to localize the peroxidase, followed by counterstain with Toluidine Blue (Sigma). Quantification of positive cells was performed on 24 sections/animal, two animals/group, three independent experiments. For double-staining secondary antibodies used were Alexa Goat anti Rabbit 594 and Alexa Goat anti Mouse 488 (Molecular Probes, Eugene, OR, USA). Sections were visualized on an Axiovert 200M microscope (Zeiss, Thornwood, NY, USA) coupled to an Apotome module.

DNA quantification

P21 hippocampus and cerebellum were manually homogenized in distilled water. DNA was pelleted with 10% TCA and centrifugation (2700 *g*, 4°C, 15 min). After the pellet was hydrolyzed with 1 N KOH and neutralized, DNA was resedimented with 5% TCA and denatured at 90°C. Samples were quantified with a diphenylamine reagent that reacts

proportionally with DNA to generate a colored reaction product that can be assessed by spectroscopy for each experiment. Sample values were converted to total DNA based on a standard curve run in parallel for each assay, as previously described (Wagner *et al.* 1999; Cheng *et al.* 2002).

Unbiased stereology

Cell number was estimated in the dentate gyrus of the hippocampus 2 weeks after MeHg exposure by using a Bioquant computerized image analysis system (Nashville, TN, USA). Color video images were obtained with the measuring system (Zeiss/Sony, Tokyo, Japan). The outlines of the brain regions were traced out at low magnification, and nuclei were counted at higher magnifications. The cell number for each region (N) was estimated by using the following algorithm: N = total number cells counted × reciprocal of section sampling fraction × reciprocal of area sampling fraction × reciprocal of thickness sampling fraction, where section sampling fraction = number section sampled/total number of sections; area sampling fraction = counting from area/grid square area; and thickness sampling fraction = optical dissector height/mean tissue thickness. Independent variance was determined by computing the percentage of variance (Var) from Nugget (Var = Nug + Estimated variance from systematic random sampling).

Western blot

Samples were obtained from P7 rats treated 8 or 24 h in the absence or presence of MeHg (5 μg/gbw) or cortical cell cultures treated 24 h with MeHg (1.5 μmol/L) and/or Z-VAD-FMK (60 μmol/L). Total cellular proteins were extracted using lysis buffer containing 1% Triton X-100, 50 mmol/L Tris–HCl, and 10 mmol/L EDTA (Falluel-Morel *et al.* 2004). The homogenate was centrifuged (20 000 g, 4°C, 15 min) and the proteins contained in the supernatant were precipitated by addition of ice-cold 10% TCA. The extract was centrifuged (15 000 *g*, 4°C, 15 min) and washed three times with alcohol/ether. The pellet was denatured in 50 mmol/L Tris–HCl (pH 7.5) containing 20% glycerol, 0.7 mol/L 2-mercaptoethanol, 0.004% (w/v) bromophenol blue, and 3% (w/v) sodium dodecyl sulfate at 100°C for 5 min, and proteins separated by 12% sodium dodecyl sulfate/polyacrylamide gel electrophoresis. After separation, proteins were electrically transferred onto a polyvinylidene difluoride membrane (Millipore, Bedford, MA, USA). The membrane was incubated with the blocking solution (1% bovine serum albumin in Tris-buffered saline containing 0.05% Tween-20) at 18°C for 1 h and revealed with antibodies against cyclin E, cyclin D1, cyclin D3 (Santa Cruz Biotechnologies, Santa Cruz, CA, USA), and cleaved caspase 3 (Cell Signaling), using a chemiluminescence detection kit (ECL System; Amersham Bioscience). Autoradiographic films were quantified using an image analysis system (Biorad, Hercules, CA, USA).

Measurement of peroxide levels

Brain peroxide levels were determined by measuring the oxidation rate of dichlorofluorescein diacetate (DCFH-DA) into the fluorescent product dichlorofluorescein. Hippocampal homogenates were diluted in Locke's buffer (154 mmol/L NaCl, 5.6 mmol/L KCl, 3.6 mmol/L $NaHCO_3$, 2 mmol/L $CaCl_2$, 10 mmol/L D-glucose, and 5 mmol/L HEPES) and incubated 15 min in darkness in the presence of 10 μmol/L DCFH-DA. Fluorescence intensity (λexc 485 nm and λem 530 nm) was read in a Spectramax M5 fluorescence plate reader (Molecular Devices, Sunnyvale CA, USA).

Spatial learning in the Morris water maze

A circular pool (180 cm diameter × 75 cm high) was filled to a depth of 45 cm with black opaque water at 22°C. The hidden platform was constructed of plexiglass (14 × 14 cm), painted black, and submerged 1.5 cm below water level. The maze was located in a 4 × 4-m

room, and extra maze cues included posters, a door, and a cage. The maze was divided in four virtual quadrants: north (N), south (S), east (E), and west (W). During the acquisition of place learning and the recovery test, the platform was in the same position (in the middle of quadrant E). During *acquisition*, there were four trials each day, and the intertrial interval was 1 min. Each animal was released from one of the quadrants S, N, or W facing the wall of the pool. The order of the release positions was varied systematically throughout the experiment as follows: day 1: S-W-N-S; day 2: N-W-S-W; day 3: W-N-S-N; day 4: N-S-N-W; day 5: W-S-N-S; day 6: S-N-W-N; and day 7: N-S-W-S. A trial ended when the rat climbed onto the platform. If a rat had not found the platform after 90 s, it was placed on the platform by the researcher. The rat was left on the platform for 30 s and then removed to its home cage under a heating lamp by the experimenter. *Memory* tests were performed 2 days and 2 weeks after the last training day, and rats were released from quadrants W and N, respectively (platform remained in quadrant E). *Motor and visual abilities* were monitored after the last recovery test by using a visual platform that protruded 2.5 cm above the surface of the water in quadrant S.

Cortical cell culture

To obtain a homogeneous population, dorsolateral cerebral cortex from E14.5 rat embryos was separated from basal ganglia and overlying meninges. Cells were mechanically dissociated, plated on 0.1 mg/mL poly-D-lysine coated culture dishes, and incubated at 37°C with 5% CO_2 in defined media (Lu and DiCicco-Bloom 1997) composed of Dulbecco's Modified Eagle's Medium and Ham's F12 medium (50 : 50 v/v; Invitrogen, Grand Island, NY, USA) and containing penicillin (50 U/mL), streptomycin (50 μg/mL), transferrin (100 μg/mL) (Calbiochem, La Jolla, CA, USA), putrescine (100 μmol/L), progesterone (20 nmol/L), selenium (30 nmol/L), glutamine (2 mmol/L), glucose (6 mg/mL), and bovine serum albumin (10 mg/mL). Unless otherwise noted, components were obtained from Sigma. Cells (3×10^5) were added to 24-well plates for [^{3}H]-thymidine ([^{3}H]-Thy) incorporation studies. Protein analysis required 4×10^6 cells plated in 60 mm dishes. Cells were plated with or without Z-VAD-FMK, and MeHg was added to the media 1 h after cell plating so that initial adhesion was not disturbed by the toxicant (Burke *et al.* 2006).

DNA synthesis *in vitro*

Plated cells were incubated with tritiated thymidine (5 lCi/mL) during the last 2h of total incubation, lifted with a trypsin-EDTA solution, and collected onto filter paper with a semi-automatic cell harvester (Skatron, Sterling, VA, USA). After addition of the luminating solution Eco-Lite (MP Biomedicals, Irvine, CA, USA), radioactivity was measured by scintillation spectrophotometry.

Statistical evaluation

A one-way ANOVA followed by Tukey–Kramer multiple comparison test was used for analysis of experiments involving three groups or more. An unpaired *t*-test with Welch's correction was used for analysis of experiments involving two groups. Data were analyzed using GraphPad Instat Version 3.05 (GraphPad Software, San Diego, CA, USA).

Results

MeHg acutely inhibits hippocampal DNA synthesis

To evaluate the effects of MeHg on developmental neurogenesis, we measured *in vivo* [^{3}H]-Thy incorporation in P7 rat hippocampus. During this post-natal period of rat development, the hippocampus is a region of active neurogenesis. Pups were treated with various doses of MeHg ranging from 2.5 to 10 μg/gbw, and [^{3}H]-Thy was used as a marker of DNA

synthesis. Evaluation of DNA synthesis was performed by using a 'percent thymidine incorporation' assay 24 h after MeHg exposure (Fig. 1a). MeHg induced a dose-dependent decrease in thymidine incorporation significant for 5 μg/gbw ($p < 0.01$) and above. This dose (5 μg/gbw) was used for all subsequent experiments. Time-course analysis indicated that MeHg inhibited DNA synthesis at 6 h and beyond, reducing incorporation by more than 20% ($p < 0.01$; Fig. 1b). To examine whether MeHg effects were specific, we compared effects in hippocampus to those in cerebellum, another structure displaying post-natal developmental neurogenesis. Whereas MeHg elicited a 44% decrease in DNA synthesis after 24 h in the hippocampus ($p < 0.001$), no effect was observed in the cerebellum (Fig. 1c). To correlate whole organ DNA synthesis to mitotic neuronal precursors, the number of S phase labeled cells in the dentate gyrus hilus was estimated, using thymidine analog, BrdU. MeHg exposure elicited a 22% reduction ($p < 0.01$) in the hilus at 24 h (Fig. 1d), and thus corresponded to the decrease in DNA synthesis (Fig. 1b). These data indicate that the toxicant decreases proliferation of neural precursor cells.

MeHg induces changes in hippocampal structure

To define the fate of cells generated during the period immediately following MeHg exposure, BrdU was injected 6 h after MeHg administration on P7, and BrdU-positive cells were assessed later at P21 by immunohistochemistry. Cells were counted in the hilus, and the granule cell and molecular layers (Fig. 2a). MeHg exposure led to a marked decrease in the number of BrdU-positive cells, by 29% in the granule cell layer ($p < 0.01$) and 22% in the hilus ($p < 0.001$), while the number of cells in the molecular layer was unaffected, suggesting that MeHg may affect specific cell layers within the dentate gyrus. The decreases in cell number may potentially produce a reduction in the size of the hippocampus. To evaluate this, total DNA content was assessed in hippocampus and cerebellum 2 weeks after treatment (Fig. 2b). Animals that were treated with MeHg on P7 had a 21% reduction in total hippocampal DNA content when compared with those injected with vehicle ($p < 0.01$). In contrast, there was no difference between groups in the cerebellum ($p = 0.84$), suggesting that during this period of life the hippocampus may be more vulnerable than the cerebellum to MeHg toxicity. Moreover, the deficits in hippocampal volume were not attributable to an overall loss of body weight after MeHg exposure (Table 1).

To further assess the layer selective effects of MeHg, the areas of the different hippocampal regions were measured (Fig. 3a). Interestingly, differences were found in the dentate gyrus, including the hilus, granule cell, and molecular layers, whereas Ammon's horn was unchanged, suggesting that cells generated weeks before perinatal exposure are less sensitive to the neurotoxic effects of MeHg. Based on these results, we analyzed cell number in the different regions of the dentate gyrus by using unbiased stereology (Fig. 3b). MeHg reduced total cell number by 16% in the granule cell layer ($p < 0.01$) and 50% in the hilus ($p < 0.001$), whereas no effects were detected in the molecular layer ($p = 0.94$). These changes in regional cell population numbers (Fig. 3b) closely paralleled differences defined previously using BrdU-labeled cell fate mapping (Fig. 2a), and thereby suggest that MeHg specifically affects neuronal precursor populations.

MeHg induces degradation of cyclin E and reductions in cyclin D1 and D3 levels

The foregoing data indicate that MeHg reduces the population of precursor cells in the hippocampus, effects that are likely mediated by changes in cell cycle regulation and/or induction of cell death. To assess the first hypothesis, we measured 24 h after MeHg exposure the hippocampal levels of several cell cycle regulators including cyclins D1, D3, and E (Fig. 4). MeHg induced a reduction in cyclin D1 (29%; $p < 0.001$; Fig. 4a), cyclin D3 (15%; $p < 0.05$; Fig. 4b), and cyclin E (31%; $p < 0.001$; Fig. 4c). In addition, the decrease in cyclin E level was associated with a twofold increase in a p18 fragment ($p < 0.001$; Fig. 4c).

This fragment is known to be the cleavage product of cyclin E catalyzed by the apoptosis-associated enzyme caspase 3 (Mazumder *et al.* 2002), suggesting that the MeHg-induced decrease in cell cycle activities may be associated with apoptosis.

MeHg induces programmed cell death and oxidative stress

Cyclin E cleavage predicted the possible occurrence of caspase 3 activation after MeHg exposure, and thus the hippocampal expression of the activated protease was studied (Fig. 5). Caspase 3 activation occurs through the cleavage of the full-length precursor, pro-caspase 3. Cleaved caspase 3 immunoreactive cells were visualized 24 h after MeHg exposure in the dentate gyrus, while protein levels were quantified by western blot analysis in whole hippocampus. In control conditions, very few caspase 3-immunopositive cells were observed in the dentate gyrus of the hippocampus (4.0 ± 1.0; mean cells per section ± SEM; Fig. 5a and c). After MeHg treatment however, a much larger number of caspase 3-positive cells was detected in the hilus and also in granule and molecular layers (56.5 ± 3.5, $p < 0.001$; Fig. 5b and d). To further quantify activation of caspase 3, we employed western blot analysis and found that MeHg induced a twofold increase in active caspase 3 levels in whole hippocampal extracts 24 h after treatment ($p < 0.001$; Fig. 5e). One metabolic pathway that can induce caspase activation and cell death is the production of reactive oxygen species (ROS), a well-known consequence of organomercurial injury to the mitochondrial oxidative chain in non-neuronal cell lines in culture (Garg and Chang 2006; Kaur *et al.* 2006). To determine whether MeHg-induced production of ROS in the hippocampus of perinatal rats, we employed the DCFH-DA oxidation assay on control and MeHg-treated animal hippocampal extracts. MeHg elicited a 26% increase in the dichlorofluorescein oxidation rate in the hippocampus ($p < 0.001$; Fig. 5f), suggesting that MeHg induced toxicity is associated with an oxidative stress process.

The effects of MeHg on DNA synthesis and cyclin E degradation are caspase dependent

The foregoing results suggest that MeHg exposure elicited both cell cycle arrest and apoptosis. To determine whether cell cycle inhibition by MeHg was a consequence of cell death, or a completely independent mechanism, the effects of MeHg on thymidine incorporation and cyclin E degradation were evaluated in the presence of the caspase inhibitor Z-VAD-FMK. This molecule inhibits all caspases by competitively binding the enzymes and preventing further cleavage of substrates. The experiment was conducted *in vitro* on cortical precursor cells for two reasons: (i) the use of Z-VAD-FMK *in vivo* raises concerns regarding access to the hippocampus after injection. Indeed, intracranial injections are required and could cause inflammatory processes with potentially confounding effects (Alessandri *et al.* 2006). (ii) Previous studies have shown that this cortical precursor culture is a suitable model for studying cellular mechanisms involved in MeHg toxicity. Cortical precursor cells were pre-treated with vehicle or vehicle plus Z-VAD-FMK (60 μmol/L) 1 h prior to the addition of MeHg. MeHg induced a 27% decrease in thymidine incorporation after 20 h (Fig. 6a), an effect previously associated with marked cell death in this model (Burke *et al.* 2006). This reduction in DNA synthesis was almost completely blocked by Z-VAD-FMK ($p < 0.05$; Fig. 6a). As blockade of caspases prevented the decrease in DNA synthesis, cyclin E levels were measured in the absence and/or presence of Z-VAD-FMK, MeHg or both. MeHg induced a 40% decrease in cyclin E levels 24 h after treatment, thereby reproducing the previous results *in vivo* (Fig. 4). In contrast, MeHg induced no change in cyclin E levels when in the presence of Z-VAD-FMK ($p < 0.05$; Fig. 6b), suggesting that apoptotic pathways play a key role in MeHg-induced toxicity and cell cycle arrest. As expected based on MeHg effects *in vivo* (Fig. 5e), MeHg induced an increase in cleaved caspase 3 levels *in vitro*, an effect that was abolished by Z-VAD-FMK coadministration (Fig. 6c). In aggregate, these studies suggest that MeHg elicits reduced

DNA synthesis by activating caspase 3 in mitotic precursors, leading to cyclin E degradation and cell death induction.

To determine whether MeHg may also elicit reduced DNA synthesis *in vivo* via apoptotic mechanisms, we sought the expression of activated caspase 3 in precursors engaged in mitotic S phase. We characterized the hippocampus at two time points, 8 and 24 h after MeHg exposure, as the kinetics of cell death are unknown (Fig. 7). In control conditions, the percentage of BrdU-labeled cells that also expressed caspase 3 was zero, whereas 8 h after MeHg exposure, 14 ± 3% of BrdU-positive cells were also caspase 3 immunoreactive, suggesting that reductions in DNA synthesis reflect, in part, death of the proliferative population. At 24 h after MeHg, a time already demonstrating a reduction in BrdU-labeled precursors (Fig. 1d), we detected no double labeling with caspase 3, suggesting that apoptosis occurring at earlier times was completed, depleting the proliferative pool at this later time.

MeHg inhibits hippocampal-dependent memory processes

The hippocampus is involved in certain types of learning, the best characterized being spatial learning (Morris *et al.* 1986). The most commonly used test for spatial learning is the Morris water maze. In this task, animals have to find a hidden platform in a pool of opaque water. Rats learn the platform location by using spatial cues outside the maze. However, rats cannot learn if the hippocampus is inactive or absent (Riedel *et al.* 1999). As our studies suggest that perinatal MeHg exposure alters normal hippocampal development, we wondered whether later emerging cognitive functions may also be affected. We first determined whether deficits in hippocampal total cell number assessed at P21 persisted until later ages. Indeed, at P35, 1 month after MeHg exposure, DNA content remained diminished to a similar degree (Fig. 8d). To assess hippocampal function, we measured performance in the water maze in rats that were exposed to MeHg ($n = 8$) or saline ($n = 9$) 7 days after birth and trained at 35 days of age. At this age, sexually dimorphic cognitive style in rats has not yet emerged (Kanit *et al.* 2000). Animals were trained to find the platform (four trials/day for 7 days; Fig. 8a). Both groups decreased their latency to find the platform across trials, but those treated with MeHg took much longer to find the platform ($p < 0.001$ on day 7/trial 4). With respect to individual differences, two out of eight MeHg-treated animals showed evidence of learning whereas eight out of the nine saline injected rats learned to escape. The memory for the platform location was assessed 2 weeks later. As expected, those that were injected with saline and that learned, remembered the platform location (mean escape latency = 21.6 s), whereas those that were injected with MeHg did not (mean escape latency = 54.5) ($p < 0.05$; Fig. 8b). The potential effects of MeHg exposure on sensory/motor processes was evaluated using a water maze task in which the platform is visible. Both groups readily found the platform using the visible cue, suggesting that MeHg exposure did not impair sensory processes used for spatial learning or motor processes involved in swimming ($p = 0.91$; Fig. 8c).

Discussion

In this study, we report that a single injection of a moderate dose of MeHg (5 μg/gbw) during the perinatal period exerts deleterious effects on rat hippocampus development and function. Indeed, MeHg induced an acute inhibition of DNA synthesis during the 24 h following the injection. This effect was associated with a dramatic increase in apoptotic cell number, and mechanistic studies indicated that cell death induction and cell cycle inhibition were caspase dependent (Fig. 9). Furthermore, these acute MeHg effects led to a significant reduction in the size of the hippocampus. Decreases in cell number were most evident in the hilus and granule cell layer of the dentate gyrus. MeHg treatment also induced a severe deficit in learning a task that depends on the hippocampus. Together, these data suggest that

exposure to one dose of MeHg during development produces rapid changes in cell birth and death, which result in structural and cognitive deficits during puberty.

Neurotoxic effects of MeHg on neonatal rat hippocampus

Our observations indicate that a single injection of MeHg in P7 rats elicits an inhibition of DNA synthesis in the hippocampus by 6 h. In contrast to hippocampus, the cerebellum appeared unaffected at this developmental stage by MeHg exposure *in vivo*, suggesting a differential sensitivity or compensatory mechanisms. In agreement with this notion, previous work performed in mice demonstrated that the cerebellum is not vulnerable to MeHg neurotoxicity during the first half of the suckling period, but becomes sensitive during the latter half (Stringari *et al.* 2006), consistent with a host of classical studies indicating proliferative effects of mercury in post-natal cerebellum (Rodier 1995).

As these acute effects of MeHg on neurogenesis could predict sustained changes in hippocampal size and structure, the consequences of MeHg exposure were investigated 2 weeks after injection. Indeed, MeHg exposure induced a 21% decrease in total hippocampal DNA content, suggesting a major reduction in total cell number. As a decrease in hippocampal size could reflect either a global reduction or a layer-specific cell loss, cell number was quantified in the dentate gyrus. Total cell number, determined by unbiased stereology, was decreased by half in the hilus and 16% in the granule layer, while no changes were observed in the molecular layer. As the hilus contains precursors to the granule cell layer neurons (Stanfield and Cowan 1979; Seress and Pokorny 1981), our observations suggest that MeHg specifically affects neuronal precursors and newly differentiated neurons, while supportive glial cells in the molecular layer appear to be less sensitive. Moreover, the size of the dentate gyrus regions were reduced, while the CA domains appeared unchanged, suggesting that the dentate gyrus which is undergoing neurogenesis is especially vulnerable. Thus acute MeHg toxicity at P7 induces sustained changes in hippocampal structure, in particular the dentate gyrus, a key structure involved in the control of learning processes (Segal and Landis 1974; Zornetzer *et al.* 1974; Seress and Pokorny 1981; Toga and Lothman 1983), potentially producing deleterious effects on cognitive processes.

Functional consequences of MeHg exposure

A single exposure of MeHg during development had dramatic effects on learning several weeks later. Hippocampal-dependent learning was assessed using the Morris water maze, in which rats use spatial cues in their environment to navigate (Morris *et al.* 1986). Animals injected with MeHg were severely impaired in their ability to use spatial cues to navigate in space. Importantly, they were not impaired in navigating when using a highly visible cue, indicating that the deficit in learning was not a result of performance deficits involving swimming or vision. Exactly how the hippocampus contributes to spatial learning and memory is unclear, although it contains cells used for navigation learning, socalled ‘place cells’ (O’Keefe 1990). It could be that exposure to the MeHg during development interferes with the development of these cells. Alternatively, it may be that MeHg depleted the pool of cells involved in hippocampal adult neurogenesis, these cells being involved in long-term memory processes (Gould *et al.* 1999; Shors *et al.* 2002; Snyder *et al.* 2005). We also observed a deficit in the long-term memory after MeHg exposure, an effect consistent with poor learning.

Mechanisms involved in MeHg-induced toxicity

As MeHg exposure reduced the levels of cyclins D1, D3, and E, we may propose that its toxicity is due to an inability to transition from the G1 to S phase of mitosis. However, the reduction of cyclin E level was associated with a twofold increase in a p18 cleavage

fragment. This fragment can be the product of proteolytic cleavage of cyclin E at Asp275 by the apoptosis-associated enzyme caspase 3 (Mazumder *et al.* 2002), suggesting that the pathway is activated. Indeed, a major role for apoptosis in MeHg-induced hippocampal toxicity is supported here by a variety of evidence including increased levels of activated caspase 3, its colocalization in mitotic cells, and reversal of mitotic inhibition and cyclin E degradation by the pan-caspase inhibitor Z-VAD-FMK (Fig. 9). Interestingly, cells were undergoing apoptosis throughout the hippocampus, including the molecular layer whose size was not modified 2 weeks later. These data suggest that glial cells may also be sensitive to MeHg toxicity, and compensate their loss through later proliferation. This is consistent with a previous study which showed that MeHg induces reactive gliosis in post-natal rat cortex (Sakamoto *et al.* 2004). Moreover, although Z-VAD-FMK has been used successfully to block caspase 3 induced damage in an adult stroke model *in vivo*, the small size of P7 pups and associated injuries of intracranial administration precluded such approaches in these current studies (Wiessner *et al.* 2000). However, the parallels in MeHg effects in our *in vitro* and *in vivo* data strongly support the proposal that the apoptotic pathway plays a major role in hippocampal damage and that caspase inhibition may be a useful strategy for therapy.

Various pathways are involved in the initiation of apoptosis (Kerr *et al.* 1972). Among these, oxidative stress may be an excellent candidate as MeHg is known to alter the mitochondrial oxidative chain, leading to the release of free radicals in cultured cells (Kaur *et al.* 2006). We extended the possible role of ROS in MeHg toxicity to this neurodevelopmental model and demonstrated that MeHg induces an increase in peroxide levels which remained elevated even until 24 h following exposure. Thus, MeHg toxicity would be mediated through a breakdown of the mitochondrial respiratory chain, leading to an increase in hippocampal peroxide levels. Sensitive cells would then execute the apoptosis program, thereby stopping cell proliferation and undergoing cell death. Consistent with this notion, it has been reported that brain regions exhibit distinct protective mechanisms against oxidative stress which could explain their differential vulnerabilities to neurotoxicants (Hassoun *et al.* 2003; Shila *et al.* 2005; Sava *et al.* 2006).

Functional implications for brain development

Chemicals in the environment can cause a wide range of human developmental disabilities, from grossly manifest to more subtle changes. They can produce subclinical deficits during development which can interact with genetic predispositions and other diseases to increase prevalence of disease states. Toxicants may also cause shifts in the distribution of cognitive test scores, and reduce the capacity to recover from other reversible conditions (Spurgeon 2006). Most importantly, given the sequence of brain development, early insults may have repercussions later on, appearing only with cognitive system maturation. Indeed, this is the scenario observed in this MeHg paradigm, in which one exposure during development induces effects on hippocampal neurodevelopment that are expressed later as deficits in mature brain function.

While unlike typical exposures in human populations, this animal model has allowed definition of the sequence of cellular and molecular events that lead to acute induction of mitotic inhibition and programmed cell death followed by alterations in hippocampal cell composition and learning behavior. Most importantly, we have now identified a highly sensitive marker for MeHg effects in the developing hippocampus, induction of activated caspase 3 immunoreactivity that increased greater than 10-fold at 24h. In turn, we are using this marker to determine the lowest MeHg dose that affects the hippocampus. In preliminary studies, we have found that a > 15-fold lower dose of MeHg (0.3 μg/gbw) elicits a threefold increase in the number of caspase 3-positive cells compared with controls (Falluel-Morel and DiCicco-Bloom, unpublished results). While our study suggests that MeHg acts on specific cellular targets such as caspase 3 to induce cell death and cell cycle exit, there are

likely additional effects on cell migration as well as axon and synapse formation (Rodier 1995; Rice and Barone 2000). Future studies will focus on even lower exposure levels and will evaluate the sequence of cellular and molecular events characterized in this model, which has been employed successfully in studying a number of endogenous and exogenous developmental factors (Jacobson 1991; Vaccarino *et al*. 1999; Adams *et al*. 2000; Kandel *et al*. 2000; Rice and Barone 2000; DiCicco-Bloom and Sondell 2005). Identification of cellular and molecular mechanisms will provide insight into pathways fundamental to brain development and critical sensitive periods and may suggest possible targets for effective intervention strategies.

Acknowledgments

This work was supported by NIH ES11256, ES05022, and USEPA R82939101. AF-M was a recipient of a Fellowship from *La Fondation pour la Recherche Médicale* (FRM-SPE20051105). KS was a recipient of a Fellowship from NIH (ES07148). We thank Kurt W. Richau for technical assistance.

Abbreviations used

[^{3}H]-Thy	[^{3}H]-thymidine
BrdU	bromodeoxyuridine
DCFH-DA	dichlorofluorescein diacetate
MeHg	methylmercury
PBS	phosphate-buffered saline
ROS	reactive oxygen species
TCA	trichloroacetic acid
Z-VAD-FMK	pan-caspase inhibitor carbobenzoxy-valyl-alanyl-aspartyl-[O-methyl]-fluoromethylketone

References

Adams J, Barone S Jr, LaMantia A, Philen R, Rice DC, Spear L, Susser E. Workshop to identify critical windows of exposure for children's health: neurobehavioral work group summary. Environ. Health Perspect. 2000; 108(Suppl. 3):535–544. [PubMed: 10852852]

Alessandri B, Nishioka T, Heimann A, Bullock RM, Kempski O. Caspase-dependent cell death involved in brain damage after acute subdural hematoma in rats. Brain Res. 2006; 1111:196–202. [PubMed: 16890922]

Burke K, Cheng Y, Li B, Petrov A, Joshi P, Berman RF, Reuhl KR, Dicicco-Bloom E. Methylmercury elicits rapid inhibition of cell proliferation in the developing brain and decreases cell cycle regulator, cyclin E. Neurotoxicology. 2006; 27:970–981. [PubMed: 17056119]

Cheng Y, Tao Y, Black IB, DiCicco-Bloom E. A single peripheral injection of basic fibroblast growth factor (bFGF) stimulates granule cell production and increases cerebellar growth in newborn rats. J. Neurobiol. 2001; 46:220–229. [PubMed: 11169507]

Cheng Y, Black IB, DiCicco-Bloom E. Hippocampal granule neuron production and population size are regulated by levels of bFGF. Eur. J. Neurosci. 2002; 15:3–12. [PubMed: 11860501]

Choi BH, Lapham LW, Amin-Zaki L, Saleem T. Abnormal neuronal migration, deranged cerebral cortical organization, and diffuse white matter astrocytosis of human fetal brain: a major effect of methylmercury poisoning in utero. J. Neuropathol. Exp. Neurol. 1978; 37:719–733. [PubMed: 739273]

DiCicco-Bloom, E.; Sondell, M. Neural development and neurogenesis. In: Sadock, BJ.; Sadock, VA., editors. Kaplan & Sadock's Comprehensive Textbook of Psychiatry. Eighth Edn. Williams & Wilkins; Philadelphia, PA: 2005. p. 33-49.

Falluel-Morel A, Aubert N, Vaudry D, Basille M, Fontaine M, Fournier A, Vaudry H, Gonzalez BJ. Opposite regulation of the mitochondrial apoptotic pathway by C2-ceramide and PACAP through a MAP-kinase-dependent mechanism in cerebellar granule cells. J. Neurochem. 2004; 91:1231–1243. [PubMed: 15569266]

Garg TK, Chang JY. Methylmercury causes oxidative stress and cytotoxicity in microglia: attenuation by 15-deoxy-delta 12, 14-prostaglandin J2. J. Neuroimmunol. 2006; 171:17–28. [PubMed: 16225932]

Gould E, Beylin A, Tanapat P, Reeves A, Shors TJ. Learning enhances adult neurogenesis in the hippocampal formation. Nat. Neurosci. 1999; 2:260–265. [PubMed: 10195219]

Hassoun EA, Al-Ghafri M, Abushaban A. The role of antioxidant enzymes in TCDD-induced oxidative stress in various brain regions of rats after subchronic exposure. Free Radic. Biol. Med. 2003; 35:1028–1036. [PubMed: 14572606]

Jacobson, M. Developmental Neurobiology. Plenum Publishing Corp; New York: 1991.

Kandel, E.; Schwartz, JH.; Jessell, TM. Principles of Neural Science. Elsevier; New York: 2000.

Kanit L, Taskiran D, Yilmaz OA, Balkan B, Demirgoren S, Furedy JJ, Pogun S. Sexually dimorphic cognitive style in rats emerges after puberty. Brain Res. Bull. 2000; 52:243–248. [PubMed: 10856821]

Kaur P, Aschner M, Syversen T. Glutathione modulation influences methyl mercury induced neurotoxicity in primary cell cultures of neurons and astrocytes. Neurotoxicology. 2006; 27:492–500. [PubMed: 16513172]

Kerr JF, Wyllie AH, Currie AR. Apoptosis: a basic biological phenomenon with wide-ranging implications in tissue kinetics. Br. J. Cancer. 1972; 26:239–257. [PubMed: 4561027]

Kolb B, Cioe J. Recovery from early cortical damage in rats, VIII. Earlier may be worse: behavioural dysfunction and abnormal cerebral morphogenesis following perinatal frontal cortical lesions in the rat. Neuropharmacology. 2000; 39:756–764. [PubMed: 10699442]

Lapham LW, Cernichiari E, Cox C, Myers GJ, Baggs RB, Brewer R, Shamlaye CF, Davidson PW, Clarkson TW. An analysis of autopsy brain tissue from infants prenatally exposed to methymercury. Neurotoxicology. 1995; 16:689–704. [PubMed: 8714873]

Lewandowski TA, Pierce CH, Pingree SD, Hong S, Faustman EM. Methylmercury distribution in the pregnant rat and embryo during early midbrain organogenesis. Teratology. 2002; 66:235–241. [PubMed: 12397631]

Lu N, DiCicco-Bloom E. Pituitary adenylate cyclase-activating polypeptide is an autocrine inhibitor of mitosis in cultured cortical precursor cells. Proc. Natl Acad. Sci. USA. 1997; 94:3357–3362. [PubMed: 9096398]

Mazumder S, Gong B, Chen Q, Drazba JA, Buchsbaum JC, Almasan A. Proteolytic cleavage of cyclin E leads to inactivation of associated kinase activity and amplification of apoptosis in hematopoietic cells. Mol. Cell. Biol. 2002; 22:2398–2409. [PubMed: 11884622]

Monfils MH, Driscoll I, Vandenberg PM, Thomas NJ, Danka D, Kleim JA, Kolb B. Basic fibroblast growth factor stimulates functional recovery after neonatal lesions of motor cortex in rats. Neuroscience. 2005; 134:1–8. [PubMed: 15951120]

Morris RG, Anderson E, Lynch GS, Baudry M. Selective impairment of learning and blockade of long-term potentiation by an N-methyl-D-aspartate receptor antagonist, AP5. Nature. 1986; 319:774–776. [PubMed: 2869411]

Myers GJ, Davidson PW. Does methylmercury have a role in causing developmental disabilities in children? Environ. Health Perspect. 2000; 108(Suppl. 3):413–420. [PubMed: 10852838]

O'Keefe J. A computational theory of the hippocampal cognitive map. Prog. Brain Res. 1990; 83:301–312. [PubMed: 2203101]

Rice D, Barone S Jr. Critical periods of vulnerability for the developing nervous system: evidence from humans and animal models. Environ. Health Perspect. 2000; 108(Suppl. 3):511–533. [PubMed: 10852851]

Riedel G, Micheau J, Lam AG, Roloff EL, Martin SJ, Bridge H, de Hoz L, Poeschel B, McCulloch J, Morris RG. Reversible neural inactivation reveals hippocampal participation in several memory processes. Nat. Neurosci. 1999; 2:898–905. [PubMed: 10491611]

Rodier PM. Developing brain as a target of toxicity. Environ. Health Perspect. 1995; 103(Suppl. 6): 73–76. [PubMed: 8549496]

Sakamoto M, Kakita A, de Oliveira RB, Pan H. Sheng, Takahashi H. Dose-dependent effects of methylmercury administered during neonatal brain spurt in rats. Brain Res. Dev. Brain Res. 2004; 152:171–176.

Sava V, Reunova O, Velasquez A, Song S, Sanchez-Ramos J. Neuroanatomical mapping of DNA repair and antioxidative responses in mouse brain: effects of a single dose of MPTP. Neurotoxicology. 2006; 27:1080–1093. [PubMed: 16831462]

Segal M, Landis S. Afferents to the hippocampus of the rat studied with the method of retrograde transport of horseradish peroxidase. Brain Res. 1974; 78:1–15. [PubMed: 4458909]

Seress L, Pokorny J. Structure of the granular layer of the rat dentate gyrus. A light microscopic and Golgi study. J. Anat. 1981; 133:181–195. [PubMed: 7333948]

Shila S, Kokilavani V, Subathra M, Panneerselvam C. Brain regional responses in antioxidant system to alpha-lipoic acid in arsenic intoxicated rat. Toxicology. 2005; 210:25–36. [PubMed: 15804455]

Shors TJ, Townsend DA, Zhao M, Kozorovitskiy Y, Gould E. Neurogenesis may relate to some but not all types of hippocampal-dependent learning. Hippocampus. 2002; 12:578–584. [PubMed: 12440573]

Snyder JS, Hong NS, McDonald RJ, Wojtowicz JM. A role for adult neurogenesis in spatial long-term memory. Neuroscience. 2005; 130:843–852. [PubMed: 15652983]

Spurgeon A. Prenatal methylmercury exposure and developmental outcomes: review of the evidence and discussion of future directions. Environ. Health Perspect. 2006; 114:307–312. [PubMed: 16451873]

Stanfield BB, Cowan WM. The morphology of the hippocampus and dentate gyrus in normal and reeler mice. J. Comp. Neurol. 1979; 185:393–422. [PubMed: 438366]

Stein J, Schettler T, Wallinga D, Valenti M. In harm's way: toxic threats to child development. J. Dev. Behav. Pediatr. 2002; 23:S13–S22. [PubMed: 11875286]

Stringari J, Meotti FC, Souza DO, Santos AR, Farina M. Postnatal methylmercury exposure induces hyperlocomotor activity and cerebellar oxidative stress in mice: dependence on the neurodevelopmental period. Neurochem. Res. 2006; 31:563–569. [PubMed: 16758366]

Tao Y, Black IB, DiCicco-Bloom E. Neurogenesis in neonatal rat brain is regulated by peripheral injection of basic fibroblast growth factor (bFGF). J. Comp. Neurol. 1996; 376:653–663. [PubMed: 8978476]

Toga AW, Lothman EW. Learning deficits after lesions of dentate gyrus granule cells. Exp. Neurol. 1983; 82:192–202. [PubMed: 6628608]

Vaccarino FM, Schwartz ML, Raballo R, Rhee J, Lyn-Cook R. Fibroblast growth factor signaling regulates growth and morphogenesis at multiple steps during brain development. Curr. Top. Dev. Biol. 1999; 46:179–200. [PubMed: 10417880]

Wagner JP, Black IB, DiCicco-Bloom E. Stimulation of neonatal and adult brain neurogenesis by subcutaneous injection of basic fibroblast growth factor. J. Neurosci. 1999; 19:6006–6016. [PubMed: 10407038]

Wiessner C, Sauer D, Alaimo D, Allegrini PR. Protective effect of a caspase inhibitor in models for cerebral ischemia in vitro and in vivo. Cell. Mol. Biol. (Noisy-le-grand). 2000; 46:53–62. [PubMed: 10726971]

Zornetzer SF, Boast C, Hamrick M. Neuroanatomic localization and memory processing in mice: the role of the dentate gyrus of the hippocampus. Physiol. Behav. 1974; 13:569–575. [PubMed: 4445274]

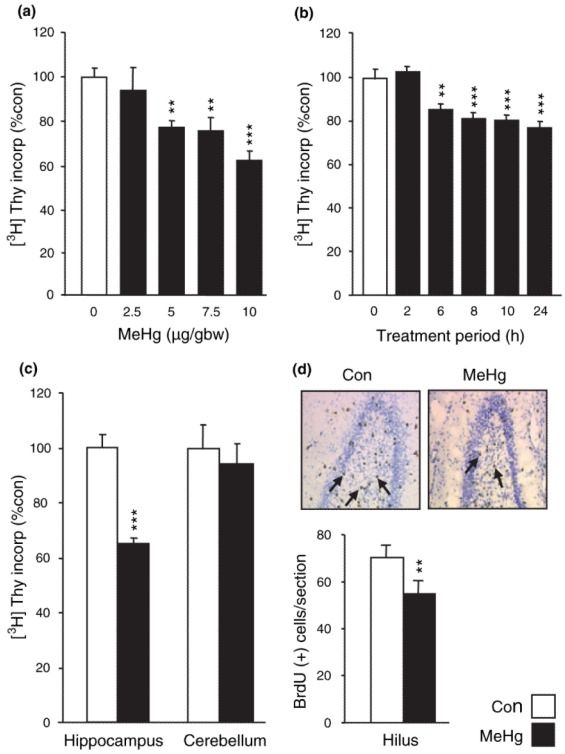

Fig. 1.

Methylmercury (MeHg) acutely inhibits DNA synthesis specifically in the hippocampus. (a) Dose-dependent effects of MeHg on [^{3}H]-thymidine ([^{3}H]-Thy) incorporation in the hippocampus. P7 rats were injected subcutaneously with vehicle or 2.5, 5.0, 7.5, or 10.0 µg/gbw MeHg at zero time, with [^{3}H]-Thy at 22 h and killed at 24 h to assess incorporation. MeHg induced a dose-dependent decrease in [^{3}H]-Thy incorporation. (b) Time course of MeHg effects on [^{3}H]-Thy incorporation in the hippocampus. P7 rats were injected with 5 µg/gbw MeHg and killed 2, 6, 8, 10, and 24 h after injection. The effect of MeHg was detectable after 6 h, and maximal at 24 h. (c) Comparison of MeHg effects in hippocampus and cerebellum. P7 rats were injected with vehicle or 5.0 µg/gbw MeHg and killed 24 h after injections. The cerebellum was not affected by MeHg, suggesting that hippocampal DNA synthesis is specifically vulnerable to organomercurials. (d) Quantification of the number of cells engaged in mitotic S-phase in the hilus of the hippocampus. P7 rats were injected with 5 µg/gbw MeHg at zero time, with bromodeoxyuridine (BrdU) 22 h later and processed at 24 h for BrdU staining. MeHg exposure diminished the number of BrdU-positive cells in the hilus of the hippocampus, suggesting a possible block in the G1/S phase transition. Pictures show representative BrdU staining in control condition and after MeHg exposure. Arrows identify BrdU-positive cells. Values are expressed as the mean ± SEM of four independent experiments for all groups, with three animals per group in each experiment. *$p < 0.05$; **$p < 0.01$; and ***$p < 0.001$ versus control.

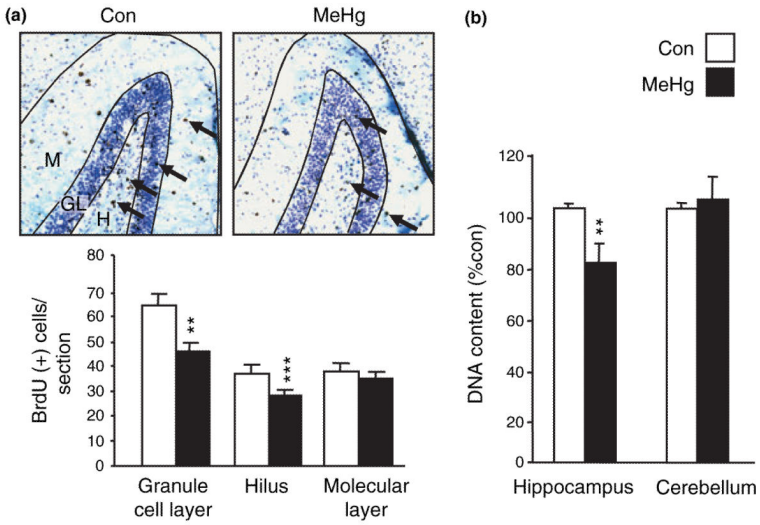

Fig. 2.

Methylmercury (MeHg) exposure induces sustained modifications of hippocampal cell number. (a) Consequences of MeHg exposure on cells that were proliferating on P7. P7 rats were injected with vehicle or 5.0 μg/gbw MeHg at zero time and with bromodeoxyuridine (BrdU) 6 h later. Animals were killed 2 weeks after injections and processed for BrdU staining. BrdU-positive cells (arrows) were counted in granule cell layer (GL), hilus (H), and molecular layer (M). The mean number of immunopositive cells per section was significantly decreased following MeHg exposure in both granule cell layer and hilus, but not in molecular layer. (b) Effect of acute MeHg exposure on later DNA content in hippocampus and cerebellum. P7 rats were injected with vehicle or 5.0 μg/gbw MeHg and killed 2 weeks after injections. Mercury exposure reduced DNA content 2 weeks later specifically in the hippocampus. $^{**}p < 0.01$ and $^{***}p < 0.001$ versus control.

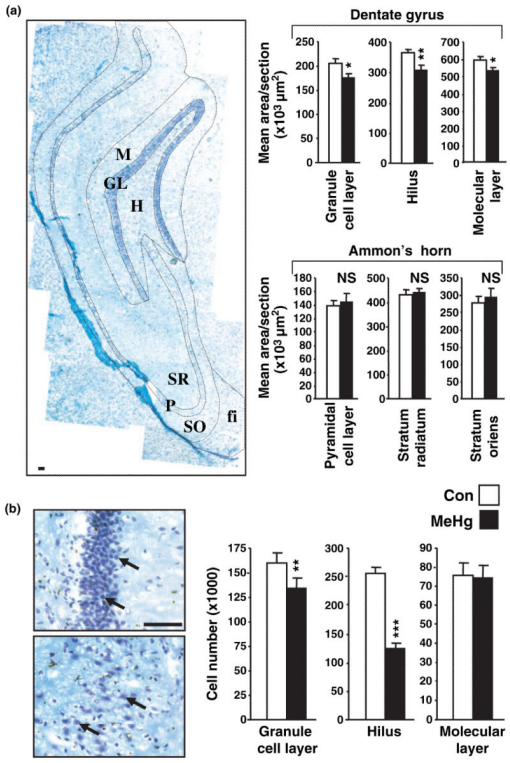

Fig. 3.

Methylmercury (MeHg) exposure affects hippocampal dentate gyrus structure and cellular composition. (a) Estimation of the size of different layers composing dentate gyrus and Ammon's horn 2 weeks after MeHg exposure. P7 rats were injected with vehicle or 5.0 μg/gbw MeHg and areas were measured using the Bioquant morphometry analysis tool. Dentate gyrus subregion sizes were reduced in the MeHg exposed group, whereas Ammon's horn was unchanged. Photomontage picture (left) shows the different hippocampal layers that were analyzed. fi, fimbria; GL, granule cell layer; H, hilus; M, molecular layer; P, pyramidal cell layer; SO, stratum oriens; and SR, stratum radiatum. Data are expressed as the mean area ± SEM per section of at least six sections per animal, three animals per group. (b) Estimation of dentate gyrus cell number 2 weeks after MeHg exposure. P7 rats were injected with vehicle or 5.0 μg/gbw MeHg and cell number was measured 2 weeks after injections in granule cell layer, hilus and molecular layer by unbiased stereology (See Materials and methods). Pictures show high magnification of cells from GL (top) and hilus (bottom). MeHg induced a decrease in cell number in granule cell layer and hilus, but not in the molecular layer, suggesting that MeHg toxicity is cell type-specific. Values are expressed as the mean cell number ± SEM per region of three independent experiments for all groups, with three animals per group in each experiment. *$p < 0.05$; **$p < 0.01$; and ***$p < 0.001$ versus control. Scale bars = 50 μm.

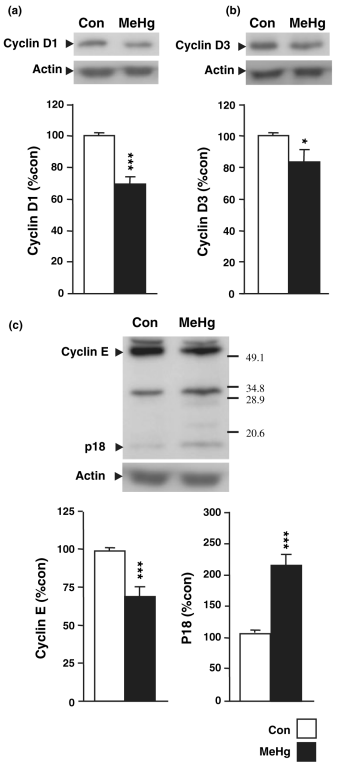

Fig. 4.

Effect of methylmercury (MeHg) on hippocampal levels of cyclin D1 (a), D3 (b), and full length and cleaved forms of cylin E (c). P7 rats were injected with vehicle or 5.0 μg/gbw MeHg and processed after 24 h for protein extraction. MeHg induced moderate decreases in levels of cyclin D1, D3, and E. Notably, the decrease in cyclin E was associated with an increase in the level of cleavage fragment p18 (c). Densitometric quantification, expressed as arbitrary units, was performed on three independent experiments, with two animals per group in each experiment. *$p < 0.05$ and ***$p < 0.001$ versus control.

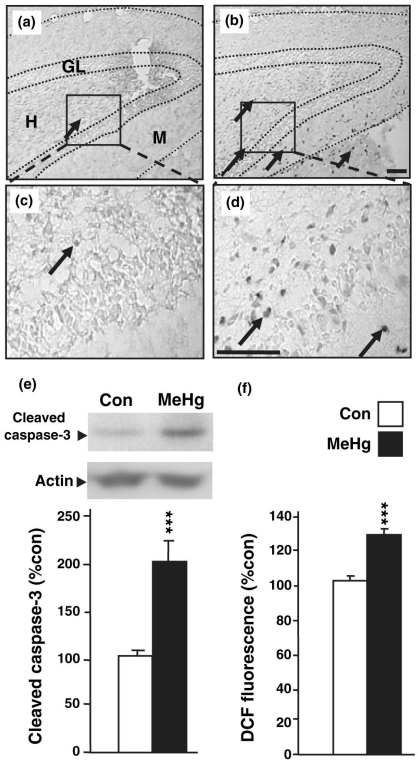

Fig. 5.

Involvement of programmed cell death in methylmercury (MeHg) -induced toxicity. (a–d) Caspase 3 immunostaining in the dentate gyrus of the hippocampus. P7 rats were injected with vehicle or 5.0 μg/gbw MeHg, killed 24 h after injections and processed for immunostaining (see Materials and methods). (a and b) Low magnification of hippocampal dentate gyrus in control (a) and MeHg-treated (b) groups. In control animals, very few caspase 3-positive cells were detected in the hippocampus, while a vastly higher number was found in MeHg-treated animals as shown by arrows. (c and d) Boxed areas in (a and b) are presented at higher magnification in (c and d), respectively. Arrows identify caspase 3-positive cells. H, Hilus of the dentate gyrus; GL, granule layer; and M, molecular layer. Scale bars = 50 μm. (e) Effect of MeHg on hippocampal levels of active caspase 3. P7 rats were injected with vehicle or 5.0 μg/gbw MeHg and processed after 24 h for protein extractions. MeHg induced a marked increase in active caspase 3 levels. Densitometric quantification, expressed as arbitrary units, was performed on three independent experiments, with two animals per group in each experiment. (f) Levels of oxidative stress in rat hippocampus following MeHg exposure. P7 rats were injected with vehicle or 5.0 μg/gbw MeHg and brain reactive oxygen species levels were determined after 24 h by measuring dichlorofluorescein (DCF) diacetate oxidation (see Materials and methods). MeHg induced a significant increase in hippocampal reactive oxygen species levels. Values are expressed as the mean DCF fluorescence ± SEM of three independent experiments for all groups, with three animals per group in each experiment. *** $p < 0.001$ versus control.

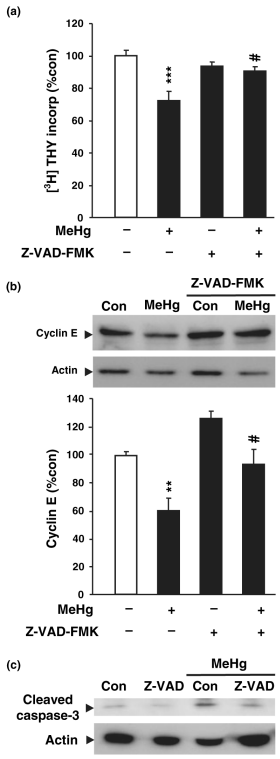

Fig. 6.

Involvement of caspases in the effect of methylmercury (MeHg) on cell cycle machinery. (a) Measurement of [^{3}H]-thymidine ([^{3}H]-Thy) incorporation in cultured neurons 20 h after treatment with MeHg (1.5 μmol/L), Z-VAD-FMK (60 μmol/L), or both. MeHg induced a decrease in thymidine incorporation which was almost completely reversed by addition of Z-VAD-FMK. Values are expressed as the mean ± SEM of five independent experiments for all groups, with four wells per group in each experiment. (b) Effect of MeHg and Z-VAD-FMK on cyclin E degradation. Western blot showing the effect of MeHg (1.5 μmol/L), Z-VAD-FMK (60 μmol/L), or both on cyclin E level. Densitometric quantification, expressed as arbitrary units, was performed on three independent experiments, with two dishes per group in each experiment. (c) Evidence of inhibitory activity of Z-VAD-FMK for MeHg-induced activation of caspase 3. Cultured neurons were treated 20 h with or without MeHg (1.5 μmol/L) and/or Z-VAD-FMK (60 μmol/L). MeHg treatment induced an increase in active caspase 3 level, which was prevented by Z-VAD-FMK. Blots were performed on two independent experiments, with two dishes per group in each experiment. $^{**}p < 0.01$ and $^{***}p < 0.001$ versus control; $^{\#}p < 0.05$ versus MeHg.

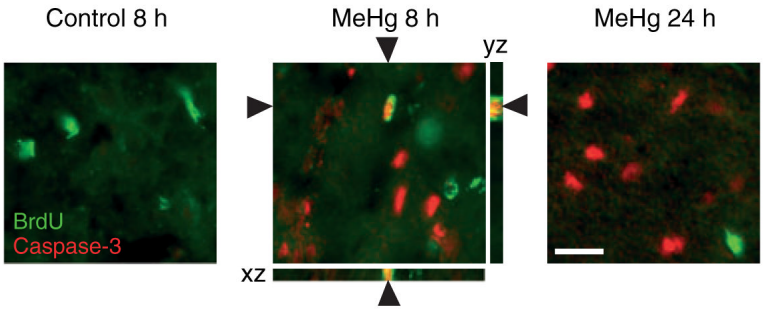

Fig. 7.

Detection of activated caspase 3 immunoreactivity in proliferative cells in the dentate gyrus following methylmercury (MeHg) exposure. P7 rats were injected with vehicle or 5.0 μg/gbw MeHg, killed at 8 and 24 h and processed for immunostaining. Double-labeling experiments demonstrate that 8 h after MeHg exposure a proportion of bromodeoxyuridine-labeled cells (green) is also caspase 3-positive (red). At 24 h, no double labeling was observed. Optical sectioning 3-dimensional analysis (Zeiss Apotome) of *XZ* and *YZ* orthogonal planes confirms colocalization of bromodeoxyuridine and caspase 3 signals. Arrowheads identify double-labeled cell. Scale bar = 25 μm.

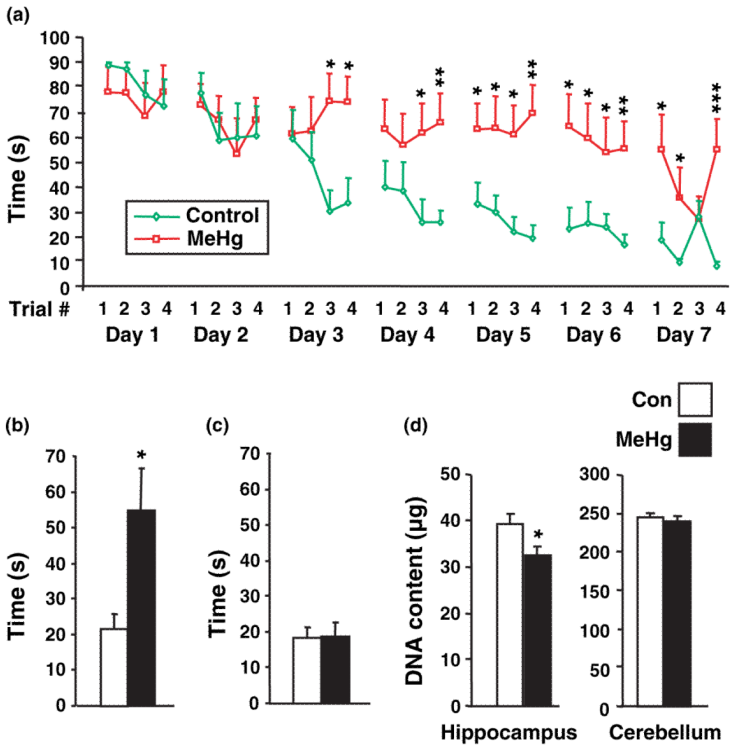

Fig. 8.

Effect of methylmercury (MeHg) on hippocampal-dependent learning processes. (a) Acquisition of place learning. P7 rats were injected with vehicle or 5.0 µg/gbw MeHg and trained at P35 four times per day to find a hidden platform in a Morris water maze (see Materials and methods). Control animals (green line) exhibited a progressive asymptotic decrease in escape latency suggesting a correct learning pattern. In contrast, the MeHg-treated animals (red line) had poor improvement of their performances. (b) Long-term recovery test. Long-term memory was measured 2 weeks later (P52) by a single trial under the same conditions as those used during training. The escape latency was twofold longer in MeHg-treated animals, suggesting that they failed to learn platform position. (c) Measurement of motor and visual abilities. Non-cognitive performances were compared by using a visible platform. No differences were found between groups suggesting that MeHg specifically alters memory processes, without damaging the animals vision and locomotion. Experiments were performed on two independent litters, with four to five animals per group in each litter. (d) Measurement of DNA content at 35 days of age. P7 rats were injected with vehicle or 5 µg/gbw MeHg and killed at P35. At the age animals were trained in water maze, hippocampal DNA was still reduced, suggesting the absence of recovery from the deficit observed at P21. *$p < 0.05$; **$p < 0.01$; and ***$p < 0.001$ versus control.

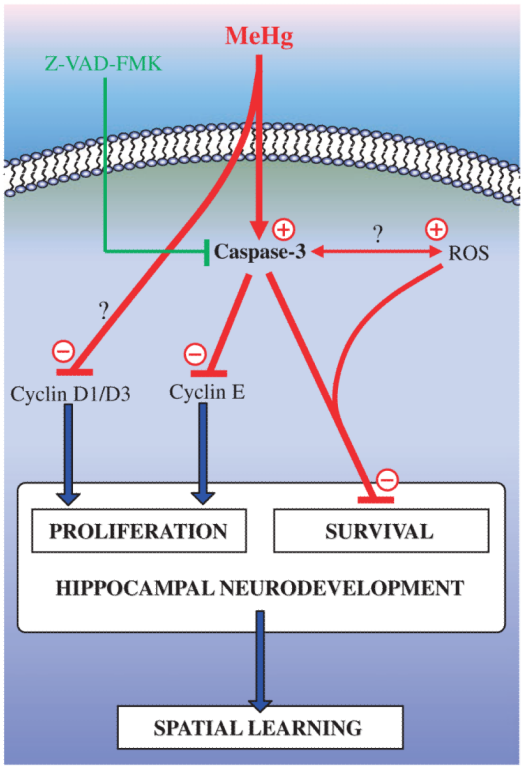

Fig. 9.

Schematic representation of the signaling mechanisms likely involved in the toxic effects of MeHg during hippocampal neurodevelopment. MeHg exposure reduces cyclin D1 and D3 levels, and degrades cyclin E through a caspase-dependent mechanism. These effects result in a cell cycle arrest at the same time as an induction of cell death. As a consequence, hippocampal neurodevelopment is altered, resulting in later abnormalities in spatial learning abilities. MeHg, methylmercury; Z-VAD-FMK, general caspase inhibitor; ROS, reactive oxygen species; ↑, activation; ⊥, inhibition. Effects of MeHg are visualized in red.

Table 1

Body weights of the animals at the ages when analyses were performed

Age (days)	8	21	35	60
Control	13.75 ± 0.29	50.36 ± 2.42	136.70 ± 2.66	340.38 ± 31.64
MeHg	13.84 ± 0.37	49.70 ± 1.44	132.08 ± 5.20	337.43 ± 28.51
p-value	0.8499	0.8169	0.4591	0.9458

Animal weights were measured prior to being killed. Values are expressed as the mean weight (g) ± SEM. MeHg, methylmercury.